

X-ray birefringence and dichroism obtained from magnetic materials

S. W. Lovesey^a and S. P. Collins^{b*}

^aRutherford Appleton Laboratory, Oxfordshire OX11 0QX, UK, and ^bDaresbury Laboratory, Cheshire WA4 4AD, UK.
E-mail: s.p.collins@dl.ac.uk

In the past decade, synchrotron radiation has triggered a surge in studies of the polarization dependence of X-ray beams passing through non-isotropic materials. A vast range of experimental results concerning polarization-dependent absorption (dichroism) and dispersion (birefringence, for example) are available from materials which are either magnetic or exhibit preferred directions due to the local atomic environment. This article aims to bring together the diversity of modern experiments in this field with established methods of optical calculus, in a way that highlights the simplicity of the underlying physics. A useful framework is formed when observable quantities, in the X-ray case, are related to atomic variables of the sample material. Atomic descriptions of absorption spectra with various levels of complexity are considered, and some well documented sum-rules are encountered. The framework is the most general allowed within the electric dipole approximation. By way of illustration, dichroic X-ray absorption by two materials with highly anisotropic properties and magnetic ions with different valence shells are considered; namely, a 3d-transition ion in ferrous niobate, and a lanthanide ion in dysprosium borocarbide. Both materials display interesting magnetic properties that are challenging to interpret at an atomic level of detail, and it is shown how absorption experiments can contribute to resolving some issues.

Keywords: birefringence; dichroism.

1. Background and orientation

The advent of modern synchrotron radiation sources has produced, in recent years, a surge in the number and variety of X-ray experiments in which the polarization of the beam reveals important information about the electronic configuration of atoms in the solid state. These have been made possible by the almost complete, often variable X-ray polarization, wavelength tunability and very high intensities available at both hard and soft X-ray synchrotron beamlines. Indeed, the wide range of dichroic effects, and the connections between them, can appear bewildering.

For each class of measurement, the challenge is to relate observable quantities – intensity, Stokes parameters *etc.* – to atomic variables and symmetries of the sample. Fortunately, the subject of polarization in optics is a mature one. An armoury of well proven theoretical tools, equally applicable at optical and X-ray wavelengths, exists in numerous texts (Swindell, 1975; Loudon, 1983; Mandel & Wolf, 1995; Brosseau, 1998). At the most fundamental level, however, the physical origin of optical constants tends to be quite different, with X-rays being sensitive primarily to the configuration of individual atoms (Thole *et al.*, 1992; van der Laan, 1994; Lovesey & Balcar, 1997). Interpretation of X-ray data therefore hinges on the relationship between atomic and optical variables, and the main goal of the present work is to develop a framework for exploring these connections.

The remainder of this paper is divided into five main sections. In §2 we relate the resonant forward-scattering amplitude to reduced dipole–dipole matrix elements *via* the Kramers–Heisenberg formula, thus providing a link between the rank-two Cartesian tensor that describes these elements, with Jones and Mueller matrices. The transmittance and polarization of X-ray photons, attenuated by a uniform anisotropic material, are thus obtained for incident beams of arbitrary partial polarization.

§3 deals with the passage of X-ray beams through materials which are magnetic and, generally, completely anisotropic. The dipole–dipole tensor is written as the sum of a scalar (giving spatially averaged properties), a symmetric tensor whose non-vanishing elements depend on the point-group symmetry of the environment of the resonant ion, and an axial vector that defines the axis of magnetic quantization. The rotational properties and eigenstates of the symmetric tensor are discussed for various symmetries, and we establish a connection between the tensor (a property only of the sample) and the 2×2 scattering matrix, from which the results of X-ray optical measurements are derived.

Atomic models for the dipole–dipole tensor vary enormously in complexity, depending on the level of detail required to describe observable quantities. §4 describes five levels of approximation, varying from a completely isotropic sample with no polarization or energy selectivity, to detailed structure in dichroic spectra arising from exchange splitting in the atomic core level. Results encompass some well documented sum-rules (Thole *et al.*, 1992; van der Laan, 1994), where tensor elements are given by various ground-state atomic moments. The paper is brought to a close with two examples, namely, ferrous niobate and dysprosium borocarbide.

2. The interpretation of experiments

2.1. The scattering length

Our treatment of the interaction of X-rays with matter is based on the Kramers–Heisenberg dispersion formula, in which the absorption process is an electric dipole ($E1$) event (Loudon, 1983; Berestetskii *et al.*, 1982). In consequence, magnetic properties of the resonant ion manifest themselves in the formula through dipole matrix-elements for the valence shell which accepts the core electron, ejected by a photon from an initially complete core level.

A photon in the beam of X-rays incident on the sample has a wavevector, \mathbf{q} , and a polarization vector, $\boldsymbol{\varepsilon}$, which is taken to be a row vector with two components. The objective of an experiment is to investigate the properties of the equilibrium state of the resonant ion, for which there are degenerate states $\{|\mu\rangle\}$. Attenuation and retardation of the X-ray beam engages quasi-discrete states, denoted here by the Greek letter η , consisting of a core level with one unfilled state and a valence shell with one additional electron. The rate of decay of such an intermediate state is γ_η/\hbar .

Let the dipole operator for the resonant ion at the position in the unit cell defined by the vector \mathbf{d} be $\hat{\mathbf{R}}(\mathbf{d})$. The strength of the $E1$ event is determined by the radial integral for the core and valence levels, R_{cl} . With this notation, the Kramers–Heisenberg formula expressed as the resonant contribution to the forward scattering length is

$$f_{\text{res}} = - (eq)^2 R_{cl}^2 \sum_{\mathbf{d}} \sum_{\eta} \left(\langle \mu | \boldsymbol{\varepsilon}' \cdot \hat{\mathbf{R}}(\mathbf{d}) | \eta \rangle \langle \eta | \boldsymbol{\varepsilon} \cdot \hat{\mathbf{R}}(\mathbf{d}) | \mu \rangle \right) / (E + E_\mu - E_\eta + i\gamma_\eta/2). \quad (1)$$

Here, it is assumed that the energy of the X-rays and the energy of the resonance are nearby, *i.e.* $E = (\hbar c q) \simeq E_\eta - E_\mu$, and the radial inte-

gral R_{cl} is the same for all intermediate states. The prime on the polarization vector denotes the transpose, and $\boldsymbol{\varepsilon}'\boldsymbol{\varepsilon}$ is a square matrix.

Let $\boldsymbol{\sigma}$ and $\boldsymbol{\pi}$ be orthogonal unit-vectors in the plane normal to the wavevector, \mathbf{q} . Taking successively $\boldsymbol{\varepsilon} = \boldsymbol{\sigma}$ and $\boldsymbol{\pi}$, and $\boldsymbol{\varepsilon}' = \boldsymbol{\sigma}' = \boldsymbol{\sigma}$ and $\boldsymbol{\pi}'$ one constructs four values of f_{res} that together form a square matrix. In the limit $\gamma_\eta = 0$, the square matrix is Hermitian and some of its properties are gathered in Appendix A of the paper. This limit is realized by working far from any resonance feature.

Our expression for f_{res} can be obtained from the scattering length, $f = f' + if''$, by equating the wave vectors for the primary and secondary beams (the forward-scattering geometry) and setting aside all contributions to f other than the one enhanced by the resonance condition. The real and imaginary parts of f satisfy a dispersion relation, also known as a Kramers–Kronig transform. The scattered intensity, f^+f , considered as a function of the states of polarization, is a 2×2 Hermitian matrix. It can be diagonalized, and the ratio of its two principal values, denoted in Appendix A by λ_+ and λ_- , gives the degree of depolarization, while their sum is proportional to the total intensity.

Attenuation (dichroism) and retardation (birefringence) in a foil are determined by the polarization dependence of its refractive index, denoted here by $n = n' + in''$. The relation between n and f is taken to be

$$n = 1 + (2\pi\rho_o/q^2)f, \quad (2)$$

in which ρ_o is the density of resonant ions present in the foil. With use of the optical theorem,

$$n'' = (2\pi\rho_o/q^2)f''_{res} = \gamma/2q, \quad (3)$$

where the attenuation coefficient, γ , has the dimensions of length⁻¹.

As a function of E , f''_{res} is a palisade of Lorentzians centred at $\Delta_\eta = (E_\eta - E_\mu)$ with a width proportional to γ_η . More than one product of dipole matrix elements will likely contribute to the weight of a Lorentzian, and for a particular resonance we need to calculate the dimensionless quantity

$$\langle Z \rangle = \sum_{\mathbf{d}} \overline{\sum_{\eta(\Delta)} (\langle \mu | \boldsymbol{\varepsilon}' \cdot \hat{\mathbf{R}}(\mathbf{d}) | \eta \rangle \langle \eta | \boldsymbol{\varepsilon} \cdot \hat{\mathbf{R}}(\mathbf{d}) | \mu \rangle)}, \quad (4)$$

where the notation $\eta(\Delta)$ indicates a sum on η restricted to intermediate states which contribute to the resonance centred at the energy Δ , and the horizontal bar denotes an average with respect to the condition of polarization.

The physical significance of $\langle Z \rangle$, defined in (4), in the interpretation of experiments can be made quite clear. For, if the dichroic signal is integrated with respect to energy, over an interval of energy that spans the intermediate states which contribute to the sum defined by $\eta(\Delta)$, then $\langle Z \rangle$ is the weight of the integrated signal, apart from unimportant factors. It is standard practice to call $\langle Z \rangle$ a sum-rule, in keeping with the Kuhn–Thomas sum-rule for oscillator strengths, and we have more to say on this subject in §4.

As we shall see in §4, use of an atomic model enables one to express $\langle Z \rangle$ in terms of the mean values of operators associated with the valence shell of the resonant ion, e.g. the mean value of the orbital angular momentum operator. The number of different operators, and hence the degree of information about the valence shell carried by $\langle Z \rangle$, depend on the extent of the sum over the intermediate states in (4). An unrestricted sum removes the entire spectrum of the intermediate states, for the closure condition is

$$\sum_{\eta} |\eta\rangle \langle \eta| = 1.$$

The corresponding expression for $\langle Z \rangle$ is devoid of explicit information about the magnetic state of the valence shell. Hence, usually an unrestricted sum of the intermediate states is not adequate for the interpretation of data.

2.2. Stokes parameters

An average of a physical quantity with respect to the condition of polarization in the primary beam of X-rays is accomplished with a density matrix, μ , whose properties are reviewed in Appendix A (in classical optics it is customary to describe polarization by a coherence matrix proportional to μ);

$$\overline{(\dots)} = \text{tr} \mu(\dots), \quad (5)$$

where tr is the trace operation. The density matrix can be expressed in the form

$$\mu = (1/2)(I + \mathbf{P} \cdot \boldsymbol{\sigma}), \quad (6)$$

where I is the unit matrix, and σ_1, σ_2 and σ_3 are Pauli matrices chosen as

$$\sigma_1 = \begin{pmatrix} 0 & 1 \\ 1 & 0 \end{pmatrix}, \quad \sigma_2 = \begin{pmatrix} 0 & -i \\ i & 0 \end{pmatrix}, \quad \sigma_3 = \begin{pmatrix} 1 & 0 \\ 0 & -1 \end{pmatrix}. \quad (7)$$

The parameters ($j = 1, 2$ and 3),

$$P_j = \text{tr}(\mu\sigma_j), \quad (8)$$

are Stokes parameters for the primary beam. While $\mathbf{P} = (P_1, P_2, P_3)$ appears as a vector in (6), it is not a vector of any standard type; in particular, \mathbf{P} is not an axial or a polar vector.

Prior to moving on, we briefly review properties of the Stokes parameters. P_1 and P_3 are measures of the linear polarization. In the right-handed and orthogonal set of coordinates $(\boldsymbol{\sigma}, \boldsymbol{\pi}, \hat{\mathbf{q}})$, P_1 describes linear polarization along directions at angles $\pm\pi/4$ to the σ -axis. The parameter P_3 describes polarization along the σ - and π -axis; $P_3 = +1$ corresponds to complete polarization in the σ -direction, and $P_3 = -1$ corresponds to complete polarization in the π -direction. The parameter P_2 measures the degree of circular polarization. Here, it is defined to be the mean value of the helicity operator. The parameters satisfy $(P_1^2 + P_2^2 + P_3^2) \leq 1$, and the equality is achieved for a completely polarized beam.

All three parameters are even with respect to the reversal of the direction of time. However, with respect to the parity operation, that changes a right-handed coordinate system to a left-handed coordinate system (and equivalent to an inversion of the coordinate system), P_1 and P_3 are unchanged while P_2 changes its sign. Hence, P_1 and P_3 behave with respect to parity as true scalar qualities. On the other hand, P_2 is not a true scalar with respect to parity and it is usual to refer to such a quantity as a pseudo-scalar. There are several arguments that quickly show that P_2 is a pseudo-scalar. For example, it is the mean helicity, and the helicity operator is the scalar product of \mathbf{q} (a polar vector) and the operator for angular momentum (an axial vector, also known as a pseudo-vector). From this definition one can see that P_2 is indeed even with respect to the reversal of the direction of time, since the helicity operator is the product of two variables that each change sign under the time-reversal operation, *i.e.* the wavevector \mathbf{q} and the operator for orbital angular momentum are odd with respect to time reversal. (The helicity and spin operators have opposite behaviour with respect to time reversal.)

2.3. Classical optics

Of central importance in the interpretation of experiments is a transmission matrix, Ω (Mandel & Wolf, 1995; Brosseau, 1998; Jones,

1948; Collins, 1999). First, the average electric energy density of the transmitted beam is proportional to

$$k = |\overline{\Omega}|^2 = \text{tr}(\Omega^+ \mu \Omega), \quad (9)$$

where Ω^+ is the Hermitian conjugate of Ω . The physical significance of (9) is made apparent on noting that the primary and transmitted complex electric fields \mathcal{E} and \mathcal{E}' , respectively, are related through $\mathcal{E}' = \mathcal{E}\Omega$, and the energy density in the transmitted beam is proportional to $(\mathcal{E}')^+ \mathcal{E}' = \Omega^+ \mathcal{E}^+ \mathcal{E}\Omega$. (NB the electric fields are row vectors.) Secondly, the Stokes parameters of the transmitted beam are ($j = 1, 2$ and 3),

$$P'_j = (1/k) \text{tr}(\Omega^+ \mu \Omega \sigma_j) = \text{tr}(\mu' \sigma_j), \quad (10)$$

where the second equality defines the density matrix of the transmitted beam, μ' . In the absence of a sample, $\Omega = I$, and any phase shift introduced by Ω is taken with respect to the unperturbed beam.

A perfect polarizer is represented by a transmission matrix which is both idempotent and singular. Physically the idempotent property of Ω refers to the fact that a beam emerging from a polarizer is unaffected by passage through a second identical polarizer. The singular property of Ω arises because the perfect polarizer destroys all information about the original state of polarization. A device which introduces a phase shift between the components of the complex electric field directed along σ and π is called a compensator. In the ideal case, there is no attenuation of the beam and a perfect compensator is represented by an Ω which is unitary.

2.4. Jones and Mueller calculus

We will express Ω in terms of a matrix which arises in the Jones calculus. Another approach to the description of optical devices uses the Mueller calculus (Brosseau, 1998). One fundamental difference between the two calculi is found in the addition of waves: Jones calculus assumes a coherent addition whereas Mueller calculus assumes an incoherent addition. A relation between the calculi, appropriate to record at this juncture, is obtained from a consideration of the Stokes parameters (8) and (10). For this purpose, let $j = 1, 2$ and 3 and define

$$s_j = s_0 P_j \quad \text{and} \quad s'_j = s'_0 P'_j, \quad (11)$$

where $k = s'_0/s_0$. In terms of the intensity parameters $\{s_h\}$ and $\{s'_h\}$ with $h = 0, 1, 2$ and 3 , the degree of polarization of the primary beam, P , is

$$P = s_0^{-1} (s_1^2 + s_2^2 + s_3^2)^{1/2} = (\mathbf{P} \cdot \mathbf{P})^{1/2},$$

and there is a similar expression for P' in terms of $\{s'_h\}$. The 4×4 Mueller matrix $\{M_{hh'}\}$ has elements

$$M_{hh'} = (1/2) \text{tr} \{ \sigma_h \Omega^+ \sigma_{h'} \Omega \}, \quad (13)$$

and it possesses the property

$$s'_h = \sum_{h'=0}^3 M_{hh'} s_{h'}. \quad (14)$$

In (13), $\sigma_0 = I$ and the three Pauli matrices are defined in (7).

From the identity $\det \mu' = (1 - P'^2)/4$ and the definition of μ' in terms of μ and Ω , we find

$$k^2(1 - P'^2) = (1 - P^2)|\det \Omega|^2 \quad (15)$$

Evidently, for the case of a completely polarized beam ($P = 1$), likewise, the beam transmitted by the sample is completely polarized. In addition we mention two cases where P' takes special values. First, the ideal polarizer always gives $P' = 1$, for in this case Ω is singular and $\det \Omega = 0$. Secondly, the ideal compensator and the ideal rotator

always gives $P = P'$, for in this case Ω is unitary, $|\det \Omega| = 1$ and $k = 1$ since $\Omega^+ \Omega = 1$. To achieve depolarization of a completely polarized beam the sample must exhibit some randomness. Such a sample is represented by some statistical ensemble of transmission matrices, not a single matrix of the type we consider. In the event that the degree of polarization in the primary beam is not complete, and $P < 1$, there is no particular constraint from (15) on the value of P' .

Bulk optical properties of a sample appear in the calculus in a 2×2 Jones matrix, denoted by \mathbf{J} , and

$$\Omega = \exp(t\mathbf{J}). \quad (16)$$

The thickness of the sample, t , is taken to be small. A real foil is modelled by a stratified unit comprised of several lamella, each possessing one desired bulk property. One can write for the Jones matrix,

$$t\mathbf{J} = bI + \mathbf{a} \cdot \boldsymbol{\sigma} = \begin{pmatrix} b + a_3 & a_1 - ia_2 \\ a_1 + ia_2 & b - a_3 \end{pmatrix}. \quad (17)$$

In general, \mathbf{a} and b are complex and the Jones matrix contains eight independent parameters (Jones, 1948). For many experiments, however, the overall phase factor does not influence the observed quantity and it can be set equal to zero leaving b purely real. An example in which the overall phase does influence the observation is two-beam interferometry (Begum *et al.*, 1986). For our part, we henceforth take b purely real, and find

$$b = -(1/2)qt(n''_{\pi} + n''_{\sigma}) = -qtn'' = -(1/2)t\gamma, \quad (18)$$

with ($j = 1, 2$ and 3),

$$a_j = -(i/2)qt\Delta n_j,$$

where $\Delta n_j = \{n(P_j) - n(-P_j)\}$ is the difference in complex refractive indices picked out by the polarization described by the Stokes parameter P_j . The relation (2) together with (18) completes the connection between bulk optical properties of the foil, described by Jones matrices, and atomic properties of the resonant ion which appear in the scattering length.

It is often convenient to use the expression, derived as described in Appendix A from (16) and (17),

$$\Omega = \exp(b)\{CI + \mathcal{S}\mathbf{a} \cdot \boldsymbol{\sigma}\}, \quad (19)$$

where $\mathcal{C} = \cosh \zeta$, $\mathcal{S} = (\sinh \zeta)/\zeta$ and $\zeta^2 = \mathbf{a} \cdot \mathbf{a}$. For the transmittance ratio and the Stokes parameters of the transmitted beam one obtains from (19),

$$k = \exp(2b)\{|\mathcal{C}|^2 + |\mathcal{S}|^2[\mathbf{a} \cdot \mathbf{a}^* + i\mathbf{P} \cdot (\mathbf{a} \times \mathbf{a}^*)] + 2\text{Re}[\mathcal{C}^* (\mathbf{P} \cdot \mathbf{a})\mathcal{S}]\}, \quad (20)$$

and ($j = 1, 2$ and 3)

$$P'_j = k^{-1} \exp(2b) \left(2\text{Re}[\mathcal{C}^* S a_j] + |\mathcal{S}|^2 \{-i(\mathbf{a} \times \mathbf{a}^*)_j - \mathbf{a} \cdot \mathbf{a}^* P_j + 2\text{Re}[a_j^* (\mathbf{a} \cdot \mathbf{P})]\} + |\mathcal{C}|^2 P_j + 2\text{Im}[\mathcal{C}^* \mathcal{S} (\mathbf{a} \times \mathbf{P})_j] \right). \quad (21)$$

The Stokes parameters P'_j do not depend on b , as one might expect. On taking the limit $t \rightarrow 0$ and retaining terms up to order t ,

$$k \rightarrow 1 - t\gamma + qt \sum_j P_j \Delta n_j'', \quad (22)$$

and

$$P'_j \rightarrow 2a'_j + P_j[1 - 2(\mathbf{a}' \cdot \mathbf{P})] + 2(\mathbf{a}'' \times \mathbf{P})_j = P_j + 2a'_j(1 - P^2) + 2[\mathbf{P} \times (\mathbf{a}' \times \mathbf{P})]_j + 2(\mathbf{a}'' \times \mathbf{P})_j. \quad (23)$$

Here, $\mathbf{a} = \mathbf{a}' + i\mathbf{a}''$, and \mathbf{a}' represents attenuation and \mathbf{a}'' represents retardation of a beam passing through a foil. It is to be noted that attenuation of a beam on passage through a foil creates polarization in the emerging beam (dichroism).

Algebra similar to that used in the derivation of (20) and (21) enables one to compute the Mueller matrix elements (13).

3. X-rays interacting with magnetic material

This section displays some general properties of attenuation and birefringence due to $E1$ (electric dipole) events in a magnetic material.

3.1. The atomic tensor

The quantity in the numerator of the Kramers–Heisenberg formula (Loudon, 1983; Berestetskii *et al.*, 1982) is made up of the product of polarization vectors $\varepsilon'_\alpha \varepsilon_\beta$, and the product of atomic matrix elements

$$T_{\alpha\beta}(\mathbf{d}) = \sum_{\eta(\Delta)} \langle \mu | \hat{R}_\alpha(\mathbf{d}) | \eta \rangle \langle \eta | \hat{R}_\beta(\mathbf{d}) | \mu \rangle, \quad (24)$$

where the notation $\eta(\Delta)$ is defined following (4), and \mathbf{d} defines the position of a resonant ion in the unit cell. In these expressions, α and β label Cartesian components of a vector. With the X-ray energy in the vicinity of a single atomic resonance at the energy Δ ,

$$f_{\text{res}}(E) = -(eq)^2 R_{\text{cl}}^2 \frac{\sum_{\mathbf{d}} \varepsilon'_\alpha \varepsilon_\beta T_{\alpha\beta}(\mathbf{d})}{(E - \Delta + i\Gamma/2)}. \quad (25)$$

The Einstein summation convention is employed, and the umbral Cartesian index is summed over its three values.

An important aspect of our $T_{\alpha\beta}$, defined by equation (24), is that there is a sum over some of the quasi-discrete intermediate states. Using an atomic model, several detailed calculations of (24) have demonstrated that it transforms as a tensor, and we will assume $T_{\alpha\beta}$ has this property. The standard argument which is used to verify the transformation property of Placzek's tensor (Berestetskii *et al.*, 1982; Gel'mukhanov & Argen, 1999), namely,

$$\sum_{\eta} \frac{\hat{R}_\alpha | \eta \rangle \langle \eta | \hat{R}_\beta}{(E + E_\mu - E_\eta)},$$

exploits the closure condition for the intermediate states. Likewise, the detailed calculations of $T_{\alpha\beta}$ to which we refer exploit the restricted sum over intermediate states in the definition (24).

In short, $T_{\alpha\beta}$ is henceforth taken to be a tensor of rank two in a space with three dimensions. Like every even rank tensor, the physical properties it describes are centrosymmetrical.

On using the Hermitian property of $\hat{\mathbf{R}}$,

$$T_{\beta\alpha}^* = T_{\alpha\beta}. \quad (26)$$

Hence, the real and imaginary parts of $T_{\alpha\beta}$, defined by $T_{\alpha\beta} = T'_{\alpha\beta} + iT''_{\alpha\beta}$, satisfy the relations

$$T'_{\alpha\beta} = T'_{\beta\alpha} \quad \text{and} \quad T''_{\alpha\beta} = -T''_{\beta\alpha}. \quad (27)$$

Next, we consider the behaviour of $T_{\alpha\beta}$ as a function of the polarity of a magnetic field, denoted by \mathbf{H} (not to be confused with the weak variable field of the photon wave). The behaviour of interest is found to follow from the assumed invariance to a change in the sign of the time variable of the equations of motion determining physical properties. A spontaneous magnetization reverses its polarity under the time-reversal operation. As far as $T_{\alpha\beta}$ is concerned, what matters is that it contains a product of two identical operators. Using \mathbf{H} to represent an applied field or a spontaneous magnetization, one finds

$$T_{\alpha\beta}(\mathbf{H}) = T_{\beta\alpha}(-\mathbf{H}), \quad (28)$$

and so

$$T'_{\alpha\beta}(\mathbf{H}) = T'_{\alpha\beta}(-\mathbf{H}), \quad T''_{\alpha\beta}(\mathbf{H}) = -T''_{\alpha\beta}(-\mathbf{H}). \quad (29)$$

The behaviour of $T''_{\alpha\beta}(\mathbf{H})$ with respect to the polarity of the field might be anticipated. For, any antisymmetrical tensor of rank two is equivalent to some axial vector, and \mathbf{H} is here an axial vector. We will use this property of an antisymmetrical tensor of rank two later in the next section.

3.2. Dichroic signals

For the product of polarization vectors we use the identity (Berestetskii *et al.*, 1982; Varshalovich *et al.*, 1988),

$$\begin{aligned} \varepsilon'_\alpha \varepsilon_\beta &= (1/3)\delta_{\alpha\beta}(\boldsymbol{\varepsilon}' \cdot \boldsymbol{\varepsilon}) + (1/2)(\varepsilon'_\alpha \varepsilon_\beta - \varepsilon'_\beta \varepsilon_\alpha) \\ &+ (1/2)[\varepsilon'_\alpha \varepsilon_\beta + \varepsilon'_\beta \varepsilon_\alpha - (2/3)(\boldsymbol{\varepsilon}' \cdot \boldsymbol{\varepsilon})\delta_{\alpha\beta}]. \end{aligned} \quad (30)$$

The identity expresses the representation of a tensor of rank two as the sum of three independent parts. The three parts are a scalar, an antisymmetrical tensor and an irreducible symmetrical tensor (the trace is zero). For the antisymmetrical tensor we employ a second identity

$$\varepsilon'_\alpha \varepsilon_\beta - \varepsilon'_\beta \varepsilon_\alpha = \varepsilon_{\alpha\beta\gamma}(\boldsymbol{\varepsilon}' \times \boldsymbol{\varepsilon})_\gamma, \quad (31)$$

where $\varepsilon_{\alpha\beta\gamma}$ is the completely antisymmetrical unit pseudo-tensor of rank three. (Under rotations of the coordinate system, the quantities $\varepsilon_{\alpha\beta\gamma}$ do not change, whereas the components of a tensor should change sign. This special property of $\varepsilon_{\alpha\beta\gamma}$ is recognized by calling it a pseudo-tensor.) Also, we define a symmetrical tensor of rank two

$$X_{\alpha\beta} = (1/2)(3/2)^{1/2}[\varepsilon'_\alpha \varepsilon_\beta + \varepsilon'_\beta \varepsilon_\alpha - (2/3)(\boldsymbol{\varepsilon}' \cdot \boldsymbol{\varepsilon})\delta_{\alpha\beta}], \quad (32)$$

with obvious property $X_{\alpha\alpha} = 0$.

Assembling the expressions in the quantity of interest one finds

$$\begin{aligned} \varepsilon'_\alpha \varepsilon_\beta T_{\alpha\beta} &= (1/3)(\boldsymbol{\varepsilon}' \cdot \boldsymbol{\varepsilon})T'_{\alpha\alpha} + (i/2)\varepsilon_{\alpha\beta\gamma}T''_{\alpha\beta}(\boldsymbol{\varepsilon}' \times \boldsymbol{\varepsilon})_\gamma \\ &+ (2/3)^{1/2}X'_{\alpha\beta}T'_{\alpha\beta}. \end{aligned} \quad (33)$$

For future purposes, it is useful to define two atomic quantities; an axial vector with components

$$\Lambda_\gamma = \frac{1}{\sqrt{2}}\varepsilon_{\alpha\beta\gamma}T''_{\alpha\beta}, \quad (34)$$

or, in components, $T''_{xy} = \Lambda_z/\sqrt{2}$ *etc.*, and, following the definition used for $X_{\alpha\beta}$, an irreducible symmetrical tensor of rank two,

$$A_{\alpha\beta} = (3/2)^{1/2}[T'_{\alpha\beta} - (1/3)\delta_{\alpha\beta}T'_{\gamma\gamma}]. \quad (35)$$

[The square root of fractions in the definitions of Λ_γ and $A_{\alpha\beta}$ arise because these quantities are Cartesian components of tensors of rank one and rank two, respectively, and the atomic matrix elements in the definition of $T_{\alpha\beta}$, from which they are constructed, are naturally calculated using spherical (atomic) tensors.]

The expression (33) is a fundamental material property. However, it cannot describe the scattering of light directly since it is three-dimensional, while light is two-dimensional (there is no component of the electric field in the direction of propagation; see, also, the discussion in Appendix A).

For the interpretation of an experiment one requires the scattering length averaged with respect to the polarization in the primary beam of X-rays. A natural choice of coordinates in which to effect the averaging is $(\boldsymbol{\sigma}, \boldsymbol{\pi}, \hat{\mathbf{q}})$. In this system of orthogonal unit vectors the polarization vectors take the values $\boldsymbol{\sigma}$ or $\boldsymbol{\pi}$, and $\varepsilon'_\alpha \varepsilon_\beta T_{\alpha\beta}$ can be

represented as a 2×2 matrix. The details are (the summation convention does not apply to σ and π),

$$\begin{aligned} \varepsilon'_\alpha \varepsilon'_\beta T_{\alpha\beta} &= (1/2)(T'_{\sigma\sigma} + T'_{\pi\pi}) \begin{pmatrix} 1 & 0 \\ 0 & 1 \end{pmatrix} + (i/\sqrt{2}) \hat{\mathbf{q}} \cdot \mathbf{\Lambda} \begin{pmatrix} 0 & 1 \\ -1 & 0 \end{pmatrix} \\ &+ \begin{bmatrix} (1/2)(T'_{\sigma\sigma} - T'_{\pi\pi}) & T'_{\sigma\pi} \\ T'_{\sigma\pi} & -(1/2)(T'_{\sigma\sigma} - T'_{\pi\pi}) \end{bmatrix}. \end{aligned} \quad (36)$$

Note that the coefficient of $\hat{\mathbf{q}} \cdot \mathbf{\Lambda}$ is proportional to the helicity operator defined in (90). The average of (36) is obtained by multiplying it by the density matrix for the polarization of the primary beam and taking the trace of the product, as in (5). For the quantity $\langle Z \rangle$, defined in (4), one finds

$$\begin{aligned} \langle Z \rangle &= \overline{\varepsilon'_\alpha \varepsilon'_\beta T_{\alpha\beta}} = \text{tr } \mu \varepsilon'_\alpha \varepsilon'_\beta T_{\alpha\beta} \\ &= (1/2) \{ T_{\sigma\sigma} + T_{\pi\pi} + P_3(T_{\sigma\sigma} - T_{\pi\pi}) \\ &\quad + iP_2(T_{\sigma\pi} - T_{\pi\sigma}) + P_1(T_{\sigma\pi} + T_{\pi\sigma}) \} \\ &= (1/2)(T'_{\sigma\sigma} + T'_{\pi\pi}) - (1/\sqrt{2})P_2(\hat{\mathbf{q}} \cdot \mathbf{\Lambda}) \\ &\quad + P_1 T'_{\sigma\pi} + (1/2)P_3(T'_{\sigma\sigma} - T'_{\pi\pi}). \end{aligned} \quad (37)$$

The dichroic signal is the part of $\langle Z \rangle$ picked out by the polarization. We see in (37) that the circular dichroic signal is proportional to $\hat{\mathbf{q}} \cdot \mathbf{\Lambda}$, and the linear (P_3) dichroic signal is proportional to $(T'_{\sigma\sigma} - T'_{\pi\pi})$.

Several comments are appropriate at this juncture. The symmetrical and antisymmetrical components of $T_{\alpha\beta}$, respectively, are even and odd under the operation which reverses the direction of time. All the Stokes parameters are even with respect to time reversal, and $\hat{\mathbf{q}}$ is odd with respect to this operation. By construction, $\mathbf{\Lambda}$ is also odd with respect to time reversal and an axial vector (also called a pseudo-vector). The properties of $\mathbf{\Lambda}$ mean that the contribution to $\langle Z \rangle$ in P_2 is indeed unchanged under the time-reversal and the parity operations.

3.3. Principal axes

Like every symmetrical tensor of rank two, $T'_{\alpha\beta}$ can be brought to diagonal form by a suitable choice of the Cartesian coordinate axes (Nye, 1960; Birss, 1964; Landau *et al.*, 1984; Schwarzenbach, 1996). Hence, there are three independent quantities in $T'_{\alpha\beta}$. There is one less independent quantity in $A_{\alpha\beta}$, constructed from $T'_{\alpha\beta}$ according to the expression (35), since it is a tensor whose trace is zero. The linear dichroic signals permit the measurement of the components $A_{\sigma\pi}$ and $(A_{\sigma\sigma} - A_{\pi\pi})$, and no other components are accessible. Shortly, we shall see that $A_{\sigma\pi}$ is obtained from $(A_{\sigma\sigma} - A_{\pi\pi})$. The coordinate axes in which $T'_{\alpha\beta}$ is diagonal have directions that are mutually perpendicular, and often they are referred to as the principal coordinate axes.

Let the principal axes be obtained from the orthogonal axes $(\sigma, \pi, \hat{\mathbf{q}})$ by a rotation specified by Euler angles α, β and γ (not to be confused with Cartesian labels) (Varshalovich *et al.*, 1988). Expression (35) is used to define rank-two atomic quantities whose mean values, $\langle A_{\alpha\beta} \rangle$, are the subject of §§4, 5 and 6. The principal axes are labelled a, b and c , and in this set of axes the matrix formed with $\langle A_{\alpha\beta} \rangle$ is diagonal. We find (Varshalovich *et al.*, 1988)

$$\begin{aligned} (3/2)^{1/2}(T'_{\sigma\sigma} - T'_{\pi\pi}) &= (A_{\sigma\sigma} - A_{\pi\pi}) \\ &= (\cos 2\alpha \sin^2 \beta)(\langle A_{cc} \rangle - \langle A_{bb} \rangle) \\ &\quad + [-\sin 2\alpha \cos \beta \sin 2\gamma \\ &\quad + \cos 2\alpha (\cos^2 \beta \cos^2 \gamma - \sin^2 \gamma)] \\ &\quad \times (\langle A_{aa} \rangle - \langle A_{bb} \rangle). \end{aligned} \quad (38)$$

The corresponding expression for $A_{\sigma\pi}$ is equal to $(A_{\sigma\sigma} - A_{\pi\pi})/2$ evaluated at the Euler angles $\alpha - \pi/4, \beta, \gamma$. The result (38) is general

in as much that the derivation does not include the traceless property of $\langle A_{\alpha\beta} \rangle$, namely, $\langle A_{\alpha\alpha} \rangle = 0$. Thus, (38) applies also to $T'_{\alpha\beta}$. It is interesting to note that, when the quantization axis (the c -axis) is aligned with the beam, which corresponds to the setting $\beta = 0$, the coefficient of $(\langle A_{aa} \rangle - \langle A_{bb} \rangle)$ in (38) reduces to $\cos 2(\alpha + \gamma)$ and the angle $\alpha + \gamma$ measures rotation about the c -axis.

3.4. Point-group symmetry

In visualizing the constraints on $T'_{\alpha\beta}$ arising from the point-group symmetry it is helpful to observe that in a space x, y, z ,

$$\varepsilon_\alpha \varepsilon_\beta T'_{\alpha\beta} = x^2 T_{xx} + 2xy T_{xy} + \dots$$

is an ellipsoid whose principal axes are those in which $T'_{\alpha\beta}$ is diagonal (Nye, 1960; Landau *et al.*, 1984). By the Neumann principle (Nye, 1960; Birss, 1964; Schwarzenbach, 1996) the ellipsoid must exhibit the symmetry of the environment of the resonant ion. Hence, $\varepsilon_\alpha \varepsilon_\beta T'_{\alpha\beta}$ is isotropic in a cubic system since the ellipsoid compatible with cubic symmetry is a sphere. For a uniaxial crystal the ellipsoid has two principal axes the same length, and in lower symmetry all three principal axes of the ellipsoid have different lengths. Fig. 1 illustrates the surface of second degree associated with cubic, tetragonal, orthorhombic and triclinic systems.

In the event that the symmetrical tensor $T'_{\alpha\beta}$ is referred to arbitrary axes (such axes are sometimes called oblique axes), the number of independent quantities is six. Principal axes are defined relative to oblique axes by three parameters, and in the principal axes $T'_{\alpha\beta}$ is specified by three independent quantities. Thus, in the latter scheme there are also six independent quantities, namely, three parameters for the specification of the principal axes relative to the oblique axes and three atomic quantities for $T'_{\alpha\beta}$. In so-called biaxial crystals (triclinic, monoclinic and orthorhombic systems) all three principal values of the tensor are different. For crystals with such a low symmetry $A_{\alpha\beta}$ is specified by two independent quantities and (38) is required in its full form. Crystals with symmetry higher than biaxial possess the property $\langle A_{aa} \rangle = \langle A_{bb} \rangle$ and, in this instance, $A_{\sigma\pi}$ and $(A_{\sigma\sigma} - A_{\pi\pi})$ are proportional to $\langle A_{cc} \rangle = -2\langle A_{aa} \rangle$ [for uniaxial crystals

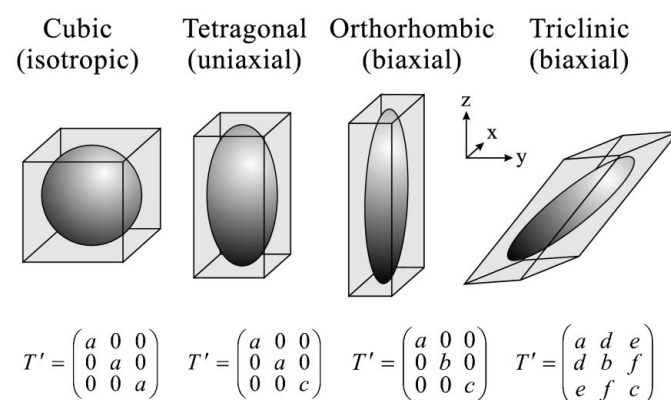


Figure 1

The ellipsoid formed by $\varepsilon_\alpha \varepsilon_\beta T'_{\alpha\beta}$ for an ion in various crystalline environments. With cubic symmetry, the ellipsoid becomes a sphere (there is no linear dichroism). An ion in a tetragonal environment has two principal axes the same length. Dichroism is observed upon rotation about any axis other than the unique axis. Orthorhombic symmetry leads to all three principal axes being different, with each being parallel to symmetry directions of the ion. Any rotation leads to dichroism and $T'_{\alpha\beta}$ has three independent elements. The final illustration shows an ion in a triclinic environment. Again, the three principal axes are of different length, but they no longer lie along symmetry directions. The tensor $T'_{\alpha\beta}$ has six independent elements, equivalent to three principal axis lengths and three angles.

(tetragonal, hexagonal and trigonal systems) the c -axis is taken to be the principal axis of symmetry of the crystal and thus $\langle A_{aa} \rangle = \langle A_{bb} \rangle$. It is perhaps useful to note that the orientation of the c -axis is independent of the Euler angle γ ; the result is

$$\mathbf{c} = (\cos \alpha \sin \beta, \sin \alpha \sin \beta, \cos \beta). \quad (39)$$

In this context, note that the coefficient of $\langle A_{cc} \rangle$ in (38) is independent of γ , and a function of α and β which is zero for $\beta = 0$ and π . Hence, for crystals with a point-group symmetry higher than biaxial, the contribution to the attenuation coefficient picked out by linear polarization (P_1 and P_3) is zero if the principal axis is parallel to the beam of X-rays. With this particular experimental geometry the linear dichroic signals from biaxial crystals can be different from zero.

By way of an example, let us consider a monoclinic (biaxial) crystal and the y -axis parallel to the twofold axis. For this case there are three independent entries in $A_{\alpha\beta}$. One finds for $A_{\alpha\beta}$,

$$\begin{pmatrix} \langle A_{xx} \rangle & 0 & \langle A_{xz} \rangle \\ 0 & \langle A_{yy} \rangle & 0 \\ \langle A_{xz} \rangle & 0 & -\langle A_{xx} + A_{yy} \rangle \end{pmatrix}$$

and

$$\begin{aligned} \varepsilon'_\alpha \varepsilon_\beta A_{\alpha\beta} &= (1/2) \langle A_{xx} + A_{yy} \rangle (\boldsymbol{\varepsilon}' \cdot \boldsymbol{\varepsilon} - 3\varepsilon'_z \varepsilon_z) \\ &+ (1/2) \langle A_{xx} - A_{yy} \rangle (\varepsilon'_x \varepsilon_x - \varepsilon'_y \varepsilon_y) + \langle A_{xz} \rangle (\varepsilon'_x \varepsilon_z + \varepsilon'_z \varepsilon_x). \end{aligned}$$

This expression takes a much simpler form in the case of a uniaxial crystal since $\langle A_{xz} \rangle = \langle A_{xx} - A_{yy} \rangle = 0$. The orientation factor $(\boldsymbol{\varepsilon}' \cdot \boldsymbol{\varepsilon} - 3\varepsilon'_z \varepsilon_z)$ is familiar as the linear dichroic term in the scattering length for magnetic scattering and absorption where the unique axis is the preferred magnetic axis.

3.5. The mean value of an atomic quantity

In the foregoing discussion use is made of angular brackets to denote the mean value of the enclosed quantity. For example, $\langle A_{aa} \rangle$ is the mean value, which is equivalent to a time average, of a component of the rank-two symmetrical tensor $A_{\alpha\beta}$, defined in (35), evaluated in the principal axes. An explicit expression is

$$\langle A_{\alpha\beta} \rangle = \sum_{\mu} p_{\mu} \langle \mu | A_{\alpha\beta} | \mu \rangle, \quad (40)$$

where p_{μ} is proportional to the thermal Boltzmann factor for the equilibrium state labelled by μ , and $\sum p_{\mu} = 1$. It is to be noted that the mean values of operators encountered in the interpretation of attenuation relate to the valence shell which accommodates the photo-ejected core electron. Details about the core level are largely removed by the sum on η in the definition of $T_{\alpha\beta}$, equation (24), and remain in $\langle Z \rangle$ only to the extent that the sum is restricted to states which contribute to a resonance labelled by quantum numbers for a core level. In general, the mean value of an atomic quantity depends on temperature, through the Boltzmann factor in (40), and all states of the ligand crystal-field appropriate to the resonant ion.

3.6. Time-reversal invariance and properties that stem from it

It is useful to record an identity for a mean value that stems from the invariance of equations of motion for material properties to a change in the direction of time (Landau & Lifshitz, 1977). Let O be any quantum mechanical operator, O^+ its Hermitian conjugate and \bar{O} the operator obtained from O by the operation of time reversal. With this notation, the identity of interest is

$$\langle O \rangle_{\mathbf{H}} = \langle \bar{O} \rangle_{-\mathbf{H}}. \quad (41)$$

All observable quantities are represented by Hermitian operators. One such case is the magnetization, \mathbf{M} , for which the operator is odd with respect to time reversal; the identity (41) yields $\mathbf{M}(\mathbf{H}) = -\mathbf{M}(-\mathbf{H})$, a result noted at the beginning of the section.

For materials in which the magnetic moments assume a spatial order, the full symmetry is obtained by adjoining elements from the point group and symmetry on reversal of all currents. The resultant space-time symmetry depends on the directions assumed by the moments, *i.e.* the spatial configuration of the magnetic moments (Birss, 1964; Landau *et al.*, 1984). In the case of ferromagnetic or ferrimagnetic configurations, consideration must be given to the influence on the configuration from any applied field. A sufficiently strong applied field can reorientate the ferromagnetic component of the magnetization. Thereby, the space-time symmetry is changed to one dictated by the direction of the applied field relative to the crystallographic axes; in fact, properties of the saturated material are governed by the structural crystal class and the direction of the applied field. Symmetry considerations are less helpful for multi-domain crystals, which possess a far lower symmetry than the structural crystal class of the material. The latter might be adequate for the interpretation of experiments on a demagnetized material.

The behaviour of the atomic quantities Λ and $A_{\alpha\beta}$ with respect to \mathbf{H} follows from their definitions in terms of the imaginary and real parts of $T_{\alpha\beta}(\mathbf{H})$. From the property (29) and the definition (34) and (35), Λ is an odd function of \mathbf{H} and $A_{\alpha\beta}$ is an even function of \mathbf{H} . In consequence, expansions of these quantities in powers of \mathbf{H} begin with Λ linear in the field and $A_{\alpha\beta}$ equal to a constant plus a correction quadratic in the field. Expressions for the atomic quantities correct at the first order in the field are, most likely, adequate, and we only need to consider Λ .

Let

$$\Lambda_{\alpha} = K_{\alpha\beta} \mathbf{H}_{\beta}, \quad (42)$$

where $K_{\alpha\beta}$ is a tensor of rank two, in general not symmetrical in the Cartesian indices. From the transformation properties of Λ_{α} and H_{β} it follows that $K_{\alpha\beta}$ is a polar tensor which is invariant (even) with respect to the operation of time reversal. $K_{\alpha\beta}$ is similar in respect to these transformations to the magnetic permeability tensor which, however, is symmetrical. There is no class of the point group for which $K_{\alpha\beta}$ is identically zero, in contrast, say, to an axial tensor of rank two.

By way of example, let us briefly consider a monoclinic system (a biaxial crystal) in which z labels the twofold axis. In this case, $K_{\alpha\beta}$ at most contains five independent quantities and it has the form

$$\begin{pmatrix} K_{xx} & K_{xy} & 0 \\ K_{yx} & K_{yy} & 0 \\ 0 & 0 & K_{zz} \end{pmatrix}.$$

The result applies to a magnetic phase of haematite, which exhibits a corundum-type crystal structure and the Fe^{3+} spins form an anti-ferromagnetic configuration (O'Handley, 2000). In the temperature range defined by the Néel temperature = 950 K and the Morin temperature = 260 K the symmetry is $2/m (C_{2h})$, and $K_{\alpha\beta}$ has the form indicated. Associated with this phase is an anisotropic exchange interaction, usually called the Dzyaloshinsky–Moriya interaction, and a small spontaneous ferromagnetism, parasitic to the anti-ferromagnetism, and perpendicular to the spin axis of the anti-ferromagnetism. Below the Morin temperature the symmetry is $\bar{3}m (D_{3d})$, and for this symmetry $K_{\alpha\beta}$ is zero apart from three elements on the diagonal and two of these are equal, $K_{xx} = K_{yy}$. Weak ferromagnetism does not coexist with the symmetry D_{3d} . In its low-

temperature phase, haematite is a fully compensated antiferromagnet and the circular dichroic signal is zero.

Many ferromagnetic materials possess a cubic crystal structure. In this instance, non-diagonal components of $K_{\alpha\beta}$ are zero and the diagonal components are equal. Hence, $\mathbf{\Lambda} = K_0 \mathbf{H}$ where K_0 is the magnitude of the diagonal components of $K_{\alpha\beta}$.

4. Atomic models for $\langle Z \rangle$

Several methods have been used to calculate the matrix elements of the dipole operators in the resonant scattering length. The methods include multiple scattering, and various computer codes for individual ions that differ in their treatment of electron correlations and the influence of the ion's environment.

Using individual ions as a starting point has proved successful in the interpretation of the magnetic properties of many materials (O'Handley, 2000), and it is adopted in this section. It has been known for a long time that algebraic results for $T_{\alpha\beta}$ can be derived (Thole *et al.*, 1992; van der Laan, 1994; Judd, 1962; Ofelt, 1962; Carra & Thole, 1994). The actual handling levied on the sum over the intermediate states in $T_{\alpha\beta}$ gives rise to different expressions for it, as we shall see. In all cases, the handling of the intermediate states makes $T_{\alpha\beta}$ a tensor, as we assumed in previous sections.

(i) A sum over all the intermediate states associated with a valence shell, and they are labelled here by η , followed by a spatial average reduces $T_{\alpha\beta}$ to a quantity proportional to the number of holes in the shell which accommodates the photo-ejected core electron. Here, and in subsequent subsections, we make explicit the dependence of $\langle Z \rangle$ on the spectrum of intermediate states it contains by writing it as $\langle Z_\eta \rangle$. Denoting the number of holes in the valence shell by n_h ,

$$\left\langle \sum_{\eta} \langle Z_{\eta} \rangle \right\rangle_{\text{av}} = (1/3) n_h. \quad (43)$$

(ii) Summing over all the intermediate states alone, and no spatial average, leads to an expression that depends on n_h and the quadrupole moment of the valence shell. The latter is a tensor of rank two, and we denote the mean value of the tensor by $\langle \mathbf{Q} \rangle$.

To give an explicit expression for the traceless and symmetrical tensor $\langle A_{\alpha\beta} \rangle$ in $\langle Z_\eta \rangle$ we need formulae that relate $\langle A_{\alpha\beta} \rangle$ to spherical components of a second-rank spherical tensor $\langle A_{\nu}^{(2)} \rangle$ where $\nu = 0, \pm 1$ and ± 2 , and we use

$$\begin{aligned} \langle A_{xy} \rangle &= (i/2)(3/2)^{1/2} \left\langle \left(A_{-2}^{(2)} - A_{+2}^{(2)} \right) \right\rangle, \\ \langle A_{xz} \rangle &= (1/2)(3/2)^{1/2} \left\langle \left(A_{-1}^{(2)} - A_{+1}^{(2)} \right) \right\rangle, \\ \langle A_{yz} \rangle &= (i/2)(3/2)^{1/2} \left\langle \left(A_{-1}^{(2)} + A_{+1}^{(2)} \right) \right\rangle, \\ \langle A_{xx} - A_{yy} \rangle &= (3/2)^{1/2} \left\langle \left(A_{+2}^{(2)} + A_{-2}^{(2)} \right) \right\rangle, \end{aligned} \quad (44)$$

and

$$\langle A_{zz} \rangle = \langle A_0^{(2)} \rangle.$$

It is interesting to note that tensors of higher rank, encountered in absorption by an electric quadrupole ($E2$) event, do not have unique relations in Cartesian and spherical coordinates (Varshalovich *et al.*, 1988).

At the second level of sophistication in handling the sum over intermediate states one arrives at the atomic quantities in $\Sigma \langle Z_\eta \rangle$. One finds

$$T'_{\alpha\alpha} = n_h \quad \text{and} \quad \mathbf{\Lambda} = 0. \quad (45)$$

The construction of $A_{\alpha\beta}$ uses the identity

$$\sum_{\alpha\beta} X_{\alpha\beta} A_{\alpha\beta} = (3/2) \mathbf{X}^{(2)} \cdot \mathbf{A}^{(2)} = (3/2) \sum_{\nu} (-1)^{\nu} X_{\nu}^{(2)} A_{-\nu}^{(2)}, \quad (46)$$

and (44) gives the rules for spherical and Cartesian components of a second-rank tensor. Our result is

$$\langle A_{\nu}^{(2)} \rangle = -2(2/3)^{1/2} \frac{1}{(2l-1)(2l+3)} \langle Q_{\nu} \rangle,$$

where l is the angular momentum of a valence shell orbital (the angular momentum of the core-level orbital is taken to be $l-1$). We therefore find

$$\begin{aligned} T'_{\alpha\beta} - (1/3) \delta_{\alpha\beta} T'_{\gamma\gamma} &= (2/3)^{1/2} \langle A_{\alpha\beta} \rangle \\ &= -\frac{4}{3(2l-1)(2l+3)} \langle Q_{\alpha\beta} \rangle, \end{aligned} \quad (47)$$

where Cartesian components of the quadrupole moment are calculated from formulae (44). The definition of $\langle \mathbf{Q} \rangle$ is such that, for $\nu = 0$,

$$\langle Q_0 \rangle \equiv \langle Q_z \rangle = (1/2) \left\langle \sum_j [3l_z^2 - l(l+1)]_j \right\rangle, \quad (48)$$

and the sum runs over all the unoccupied states in the valence shell. The remaining four components of $\langle Q_{\nu} \rangle$, with $\nu = \pm 1$ and ± 2 , contain the reduced matrix element in $\langle Q_0 \rangle$, *i.e.* the Wigner-Eckart theorem applies to every contribution to $\langle Q_{\nu} \rangle$ (Landau & Lifshitz, 1977).

(iii) At the next level of sophistication in handling the sum over the intermediate states, η is restricted to states that contribute to a resonance labelled by the total angular momentum of the core level, \vec{J} ; $\vec{J} = \vec{l} \pm \frac{1}{2}$ and $\vec{l} = l - 1$. If we denote the mean value of the energy at which the resonance is observed by Δ , the notation $\Sigma_{\eta(\Delta)}$ means a sum on η restricted to the states that contribute to the structure around $\Delta = \Delta(\vec{J})$. The value of

$$\sum_{\eta(\Delta)} \langle Z_{\eta} \rangle$$

is the weight of the integrated absorption signal, and the following expressions include results from the first investigation of the associated sum-rule (Thole *et al.*, 1992; van der Laan, 1994; Carra & Thole, 1994).

One finds

$$T'_{\alpha\alpha} \equiv \sum_{\alpha=x,y,z} T'_{\alpha\alpha} = \frac{l}{(2l+1)} n_h, \quad (49)$$

$$\mathbf{\Lambda} = \frac{1}{(2l+1)\sqrt{2}} \langle \mathbf{L} \rangle, \quad \text{with} \quad T'_{xy} = \frac{\langle L_z \rangle}{2(2l+1)} \quad \text{etc.} \quad (50)$$

and

$$T'_{\alpha\beta} - (1/3) \delta_{\alpha\beta} T'_{\gamma\gamma} = -\frac{2}{3(4l^2-1)} \langle Q_{\alpha\beta} \rangle, \quad (51)$$

where the quadrupole tensor is defined in (ii).

At the third level of sophistication, the forward scattering-length reveals information on the orbital contribution, $\langle \mathbf{L} \rangle$, to the magnetic moment carried by the valence shell. The coefficient of P_2 in (37) is

$$-\frac{1}{2(2l+1)} \hat{\mathbf{q}} \cdot \langle \mathbf{L} \rangle.$$

In other words, the circular dichroic signal is sensitive to the projection onto the direction of the X-ray beam of the orbital moment. In the case of $3d$ transition ions it is customary to define $\langle \mathbf{L} \rangle = (g_o - 2) \langle \mathbf{S} \rangle$, where g_o is the gyromagnetic factor and \mathbf{S} is the total spin operator for the valence shell. Lanthanide ions are distinguished by a very strong spin-orbit interaction in the valence shell,

and $\mathbf{J} = \mathbf{L} + \mathbf{S}$ is a good quantum number (to a very good approximation). The Landé factor, g , satisfies $g\mathbf{J} = (\mathbf{L} + 2\mathbf{S})$, and $\mathbf{L} = (2 - g)\mathbf{J}$.

(iv) The spin-orbit coupling on the core level makes \bar{J} a good quantum number and the states $\bar{J} = \bar{l} \pm \frac{1}{2}$ have different energies. In consequence, with sufficient resolution in energy, it is possible to investigate the absorption at the two spin-orbit split partners. The weights for the partners are

$$\sum_{\eta(\pm)} \langle Z_{\eta} \rangle$$

and one finds (Lovesey & Balcar, 1997)

$$T'_{\alpha\alpha} = \frac{1}{2} \frac{l}{(4l^2 - 1)} \left[(2\bar{J} + 1)n_h \pm 4 \left(\frac{l-1}{l} \right) \langle \Sigma s \cdot \mathbf{l} \rangle \right], \quad (52)$$

where $\langle \Sigma s \cdot \mathbf{l} \rangle$ is the mean value of the spin-orbit operator,

$$\Lambda = \frac{1}{2\sqrt{2}} \frac{1}{(4l^2 - 1)} \times \left\{ (2\bar{J} + 1) \langle \mathbf{L} \rangle \pm (4/3)(l-1)[l \langle \mathbf{S} \rangle + (2l+3) \langle \mathbf{T} \rangle] \right\}, \quad (53)$$

and

$$\langle A_v^{(2)} \rangle = -\frac{1}{\sqrt{6}} \frac{1}{(2l-1)^2(2l+1)} \left\{ (2\bar{J} + 1) \langle Q_v \rangle \pm (4/5)[(l-1)(2l-1) \langle P_v \rangle + 3 \langle R_v \rangle] \right\}. \quad (54)$$

Recall that in the principal axes the two independent quantities in the traceless and symmetrical tensor $A_{\alpha\beta}$ depend only on $\langle A_0^{(2)} \rangle$ and $\langle A_{\pm 2}^{(2)} \rangle$. When summed over the two values of \bar{J} the foregoing expressions for $T'_{\alpha\alpha}$, Λ and $\langle A_v^{(2)} \rangle$ reduce to the expression in (iii), as expected.

The rank-one operator \mathbf{T} (not to be confused with the tensor $T_{\alpha\beta}$) and the rank-two operators \mathbf{P} and \mathbf{R} are completely specified by the expressions

$$\langle T_0 \rangle \equiv \langle T_z \rangle = -\left\langle \sum_j \left[3\hat{R}_z(\hat{\mathbf{R}} \cdot \mathbf{s}) - s_z \right] \right\rangle, \quad (55)$$

$$\langle P_0 \rangle = (1/2) \left\langle \sum_j \left[3s_z l_z - \mathbf{s} \cdot \mathbf{l} \right] \right\rangle, \quad (56)$$

$$\langle R_0 \rangle = -(1/2) \left\langle \sum_j \left\{ [2l(l+1) + 1] s_z l_z + [l(l+2) - 2] \mathbf{s} \cdot \mathbf{l} - 5l_z(\mathbf{s} \cdot \mathbf{l}) l_z \right\} \right\rangle. \quad (57)$$

Values of $\langle \mathbf{T} \rangle$, $\langle \mathbf{P} \rangle$ and $\langle \mathbf{R} \rangle$ for a $3d$ -transition ion are given in the next section.

(v) The spin projection of the core state, \bar{M} , can take $(2\bar{J} + 1)$ values. The degeneracy of the states labelled by \bar{M} is removed by the exchange field acting on the core level. To take this fine structure into account one needs the weights

$$\sum_{\eta(\bar{M})} \langle Z_{\eta} \rangle.$$

For each weight there is in f''_{res} one Lorentzian function of energy, *i.e.* the energy dependence of a spin-orbit split partner is modelled by $(2\bar{J} + 1)$ Lorentzian functions. We shall not give the corresponding expressions for $T'_{\alpha\alpha}$, Λ and $\langle A_v^{(2)} \rangle$ simply because they are lengthy. Examples of the expressions appropriate for a $3d$ ion and a lanthanide ion are found in Lovesey & Balcar (1997), Lovesey *et al.* (1998).

5. Example: ferrous niobate

The transition-metal niobates crystallize in the columbite structure, which is an orthorhombic system and thus biaxial. The space group is $Pbcn$ (D_{2h}^{14}). Below 4.9 K, ferrous niobate exhibits antiferromagnetic order with a canted spin configuration which is illustrated in Fig. 2. For a fully compensated spin configuration the circular dichroic signal is zero. A non-zero signal can be created by application of the magnetic field. In the case of ferrous niobate at 2.0 K the field-induced magnetization is significant for modest fields and two field-induced configurations of magnetic moments are included in Fig. 2. The critical value of the magnetic field and the magnetization depends on the orientation of the applied field relative to the crystal axes. The anisotropy in the magnetization is mirrored in the gyromagnetic factors; in the principal axes, the gyromagnetic tensor of the ferrous ion has values $g_a = 2.0$, $g_b = 2.37$ and $g_c = 3.09$.

The results given below are based on a model of ferrous niobate in which the degrees of freedom of the orbital angular momentum of the ferrous ion are explicitly taken into account (Heid *et al.*, 1996). The model is consistent with a wealth of experimental data, including the magnetization, susceptibility and neutron diffraction pattern of a single crystal.

5.1. Atomic quantities

To obtain the results of this subsection, the wave function of the ferrous ion is calculated by perturbation theory, correct to the first order in the spin-orbit coupling. The mean values of the atomic

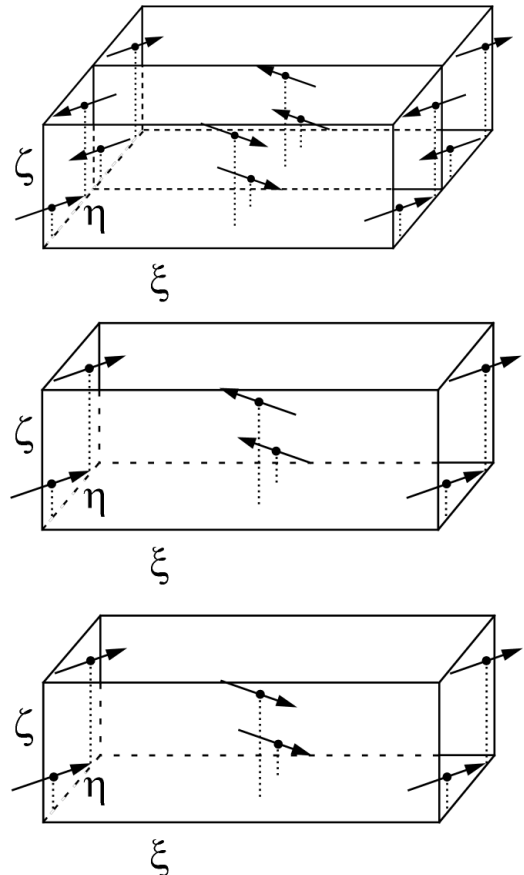


Figure 2 The magnetic structures of FeNb_2O_6 , showing the antiferromagnetic phase (top), and high-field phases with magnetization along the ζ -axis (middle) and the ξ -axis (bottom). All moments lie in the ξ - ζ plane. (From Heid *et al.*, 1996.)

quantities, introduced in 4(iv), are correct to the same order of approximation (Lovesey & Grimmer, 1997). Results are appropriate for dichroic signals observed near the Fe L_2 and L_3 absorption edges.

We begin with the atomic quantities in \mathbf{A} , equation (53). In the principal axes, (a, b, c), one finds

$$\langle L_c \rangle = (g_c - 2)\langle S_c \rangle \quad (58)$$

and

$$\langle T_c \rangle = (1/14)[1 - (3/4)(g_b - 2)]\langle S_c \rangle. \quad (59)$$

Because $(g_a - 2) = 0$ there is no contribution to the anisotropy tensor, $\langle \mathbf{T} \rangle$, from the component of the moment in the \mathbf{a} -direction. The remaining Cartesian components of \mathbf{A} are zero. Using the values quoted for the gyromagnetic factors $\langle T_c \rangle = 0.047\langle L_c \rangle$. [Results for $\langle \mathbf{T} \rangle$ for other 3d-transition ions are found in Lovesey & Balcar (1997), Saintavit *et al.* (1995) and Crocombette *et al.* (1996).]

The quadrupole moment, which appears in the symmetrical tensor $A_{\alpha\beta}$, is independent of the temperature. The spherical components $\langle Q_v \rangle$ different from zero are $\langle Q_0 \rangle = 3/2$ and $\langle Q_{\pm 2} \rangle = -(3/2)^{3/2}$, and these particular values are indicative of the main component of the ground-state orbital, which is the $|yz\rangle$ orbital in the Γ_5 triplet. Thus, in the paramagnetic phase the symmetrical tensor $\langle A_{\alpha\beta} \rangle$ is different from zero, unlike \mathbf{A} .

The remaining rank-two tensors depend on temperature through $\langle S_c^2 \rangle$. One finds

$$\langle P_0 \rangle + \langle R_0 \rangle = -(5/4)\{(g_c - 2)\langle S_c^2 \rangle + (1/4)(g_b - 2)[\langle S_c^2 \rangle - S(S+1)]\}, \quad (60)$$

and

$$\langle P_{\pm 2} \rangle + \langle R_{\pm 2} \rangle = (5/16)(3/2)^{1/2}(g_b - 2)[S(S+1) - \langle S_c^2 \rangle], \quad (61)$$

where $S = 2$ is the spin of the ferrous ion.

Combining the results for $\langle \mathbf{Q} \rangle$, and $(\langle \mathbf{P} \rangle + \langle \mathbf{R} \rangle)$ in (55) and using (45), we arrive at expressions for the quantities in the dichroic signal picked out by linear polarization, namely

$$\sqrt{6} \langle A_{cc} \rangle = (1/30)\{- (2\bar{J} + 1) \pm 2[(g_c - 2)\langle S_c^2 \rangle + (1/4)(g_b - 2)(\langle S_c^2 \rangle - S(S+1))]\}, \quad (62)$$

and

$$\sqrt{6} \langle A_{aa} - A_{bb} \rangle = (1/10)\{(2\bar{J} + 1) \pm (1/2)(g_b - 2)(\langle S_c^2 \rangle - S(S+1))\}. \quad (63)$$

These expressions control the coefficient of P_3 in $\langle Z \rangle$, found in (37). The dependence on temperature of the linear dichroic signal is not simple; in particular, the signal is not proportional to $\langle S_c^2 \rangle$. In the limit of an infinite temperature, $\langle S_c^2 \rangle \rightarrow S(S+1)/3$, and the approach to this value depends on the strong uniaxial magnetic anisotropy in ferrous niobate. A value of $\langle A_{aa} - A_{bb} \rangle$ different from zero reflects the low symmetry of the crystal. Another point to note is that the linear dichroic signal is not zero for a fully compensating antiferromagnetic configuration of the moments, whereas the circular dichroic signal is zero for such a configuration. The geometrical factor in the circular dichroic signal is simple, being the projection of \mathbf{A} on the direction of propagation of the X-ray beam. When the projection is zero the linear dichroic signal is non-zero. The general rules for dichroic signals are illustrated by considering three phases of ferrous niobate.

5.2. Spontaneous magnetic order in zero applied field

In this phase the sum in (25) over the eight ferrous ions in the magnetic unit cell can be different from zero for spherical tensors of even rank. A spherical tensor of rank one does not contribute to the sum and, as expected, there is no circular dichroic signal for a fully compensating antiferromagnet.

Let us consider an experimental geometry in which the beam of X-rays is directed along one of the crystal axes ξ, η and ζ . The twofold axis of rotation that passes through a ferrous ion runs along the η -axis. In the ordered state, moments lie in the ξ - ζ plane and the canting angle φ is with respect to the ζ -axis. Assuming this axis and the beam are parallel, the linear dichroic signal in $\langle Z \rangle$ obtained from (37) is

$$+P_3 2\sqrt{6} \{ \sin^2 \varphi \langle A_{cc} \rangle + (1/3)(1 + \cos^2 \varphi) \langle A_{aa} - A_{bb} \rangle \}, \quad (64)$$

and we look to (63) for the atomic quantities entering this result.

5.3. Field-induced moment along the ζ -axis

Beyond a critical value, a magnetic field applied along the ζ -axis induces a new configuration of the moments, illustrated in Fig. 2, that can be described in terms of the chemical unit cell. In this phase, the sum over ions in (25) can be different from zero for spherical tensors of even and odd rank.

By way of an interesting example, we calculate the circular dichroic signal obtained with the field parallel to the ζ -axis and directed along the beam. The component of interest in (37) is found to be

$$-(2/15)P_2 \cos \varphi \{ (2\bar{J} + 1) \langle L_c \rangle \pm (4/3)[2\langle S_c \rangle + 7\langle T_c \rangle] \}, \quad (65)$$

where \bar{J} is the total angular momentum of the $2p$ core state. With increasing applied field, φ approaches zero. Using (58) and (59), the signal (65) is proportional to the spin moment which depends on the magnitude of the applied field and temperature.

5.4. Field-induced moment along the ξ -axis

With the crystal held at a temperature of 2 K the critical field for the ξ -axis is 9.0 kOe, which is just half the value of the critical field for the ζ -axis. The field-induced configuration of moments is included in Fig. 2. If we adopt the experimental geometry used in the two previous examples the induced moment is perpendicular to the beam of X-rays, and the circular dichroic signal is zero. The linear dichroic signal is described by (64) and at saturation $\varphi = \pi/2$.

Let us consider the applied field inclined at an arbitrary angle with respect to the beam. The angle ψ is zero for ζ and the beam aligned, leaving the field applied along ξ at right angles to the beam. The circular dichroic signal in $\langle Z \rangle$ is found to be

$$(2/15)P_2 \sin \psi \sin \varphi \{ \dots \}, \quad (66)$$

where the curly brackets contain the atomic quantities appearing in (65). As predicted, the circular dichroic signal is zero when the induced moment is perpendicular to the beam.

Experiments of the type described, where one tracks dichroic signals as a function of the magnitude and direction of an externally applied magnetic field, will certainly provide valuable new insight into the microscopic nature of magnetocrystalline anisotropy.

6. Example: dysprosium borocarbide

The tetragonal lanthanide compound DyB_2C_2 (dysprosium borocarbide) has recently attracted attention because some of its properties are consistent with an antiferroquadrupole (AFQ) configuration. On the basis of specific heat, magnetization and

neutron diffraction measurements on a single crystal, Yamauchi *et al.* (1999) proposed that an AFQ configuration exists between $T_Q = 24.7$ K and $T_C = 15.3$ K, below which there is long-range magnetic order. A plausible model of features that set in at T_Q involves two almost degenerate Kramers conjugate Dy states well separated in energy from the other 12 crystal-field states created from ${}^6\text{H}_{15/2}$. Orbital degrees of freedom in the doublet might contrive at T_Q to produce a phase transition and long-range ordering of the $4f$ quadrupoles, with no accompanying magnetization anomaly, followed at T_C by ferromagnetic ordering of the $4f$ moments.

Two groups of researchers, using resonant X-ray Bragg diffraction near the Dy L_3 edge, have reported compelling evidence in favour of an AFQ configuration (Tanaka *et al.*, 1999; Hirota *et al.*, 2000). However, not all issues are settled. We will show in this section that dichroic signals from DyB₂C₂ obtained at the Dy M_4 and M_5 absorption edges could provide additional information to fuel the debate about its unusual electronic and magnetic properties.

At room temperature the tetragonal structure of DyB₂C₂ belongs to the space group $P4/m\bar{b}m$. Below T_Q the crystal adopts a lower symmetry for which Tanaka *et al.* (1999) have proposed the space group $P4_2/mnm$, with dysprosium ions occupying sites $4(c)$ that have symmetry $2/m$. In consequence, the value of $\langle A_{\zeta\zeta} \rangle$ is the same for every Dy ion and the quadrupole ordering is revealed in the relative signs of $\langle A_{\xi\xi} - A_{\eta\eta} \rangle$ and $\langle A_{\xi\eta} \rangle$. One finds that for neighbouring ions along the ζ -axis, ions are rotated by $\pi/2$ about the ζ -axis with respect to one another, that components $\langle A_{\xi\xi} - A_{\eta\eta} \rangle$ and $\langle A_{\xi\eta} \rangle$ are equal in magnitude and opposite in sign. Neighbouring ions in the plane normal to the ζ -axis are related by reflection in the $\xi = \eta$ plane, and this symmetry leads to $\langle A_{\xi\eta} \rangle$ all of one sign and $\langle A_{\xi\xi} - A_{\eta\eta} \rangle$ of opposite sign. The Bragg diffraction structure factor evaluated for space-group allowed reflections, which include forward scattering (*i.e.* absorption), contains $\langle A_{\zeta\zeta} \rangle$ and not any other component of $\langle A_{\alpha\beta} \rangle$ mentioned. The latter contribute to the structure factor for space-group forbidden reflections and give rise to Templeton–Templeton scattering observed by Hirota *et al.* (2000). The intensities of these forbidden reflections depend on the orientation in the ξ – η plane of the major axis of the quadrupole moment which need not be the same as the magnetic canting angle φ . All these findings follow from the properties of the space group assigned to DyB₂C₂ and experimental verification of any one builds confidence in it.

Looking at Fig. 3, the magnetic Dy principal axis lies in a plane normal to the twofold symmetry axis (ζ -axis) and it subtends an angle φ with the crystal ξ -axis. If we denote the principal axis of a reference ion as $(\cos\varphi, \sin\varphi, 0)$, the principal axes of the three remaining dysprosium ions in the unit cell are $(-\sin\varphi, -\cos\varphi, 0)$, $(-\sin\varphi, \cos\varphi, 0)$ and $(\cos\varphi, -\sin\varphi, 0)$. In this case, below T_C the net moment is directed along the ξ -axis and it vanishes should $\varphi = 45^\circ$. We take $(\cos\varphi, \sin\varphi, 0)$ to be the z -axis in local (orthogonal) principal axes (x, y, z) and choose to have x directed along the twofold symmetry axis.

The crystal axes (ξ, η, ζ) are obtained from the experimental axes (σ, π, \hat{q}) by rotations specified by Euler angles α, β and γ (Varshavovich *et al.*, 1988); in §3.3 we used a similar description for crystal principal axes. Referred to the experimental axes, the ζ -axis in terms of Euler angles is given by (39). The ξ and η axes depend on the Euler angle γ , and for the ξ -axis one finds

$$\xi = (\cos\alpha \cos\beta \cos\gamma - \sin\alpha \sin\gamma, \sin\alpha \cos\beta \cos\gamma + \cos\alpha \sin\gamma, -\cos\gamma \sin\beta). \quad (67)$$

From (37) and §4(iv) the circular dichroic signal is found to be

$$(1/70)P_2 \sin\beta \cos\gamma (\cos\varphi - \sin\varphi) \{ (2\bar{J} + 1)\langle L_z \rangle \pm 8[\langle S_z \rangle + 3\langle T_z \rangle] \}, \quad (68)$$

where \bar{J} is the total angular momentum of either the M_4 or M_5 core state. The signal is proportional to the net moment and vanishes for $\beta = 0$ because in this setting the moment is perpendicular to the beam of X-rays. With regard to the dependence of (68) on γ note that with $\beta = \pi/2$ the angle γ describes the inclination of the net moment, directed along the ξ -axis, with respect to the beam.

For the linear dichroic signal we find

$$P_3 (3/2)^{1/2} \cos 2\alpha \sin^2\beta \{ -\langle A_{zz} \rangle + \langle A_{xx} - A_{yy} \rangle \}, \quad (69)$$

where the quantities $\langle A_{xx} \rangle$ *etc.* are obtained from (44) and (54). Inspection of (54) reveals that the linear dichroic signal offers direct access to the Dy quadrupole moments, and other similar quantities that described the anisotropy of the $4f$ valence shell.

Evidently, the circular and linear dichroic signals yield separate information about quadrupole and magnetic configurations. Signals predicted by (68) and (69) convey the model adopted for DyB₂C₂, in which the magnet unit cell contains four dysprosium ions with easy magnetic axes arranged, as illustrated in Fig. 3, in the plane normal to the $2/m$ axis at angles $\varphi, 90^\circ - \varphi, 90^\circ + \varphi$ and $-\varphi$.

By way of orientation to the size of the atomic quantities in the dichroic signals we give values appropriate for a fully saturated dysprosium ion with $\langle J_z \rangle = 15/2$, $\langle L_z \rangle = (2 - g)\langle J_z \rangle = 5$ and $\langle S_z \rangle = (g - 1)\langle J_z \rangle = 5/2$. For this state one finds $\langle T_z \rangle = -1/3$ and a circular dichroic signal

$$(1/14)P_2 \sin\beta \cos\gamma (\cos\varphi - \sin\varphi) \{ (2\bar{J} + 1) \pm (12/5) \}.$$

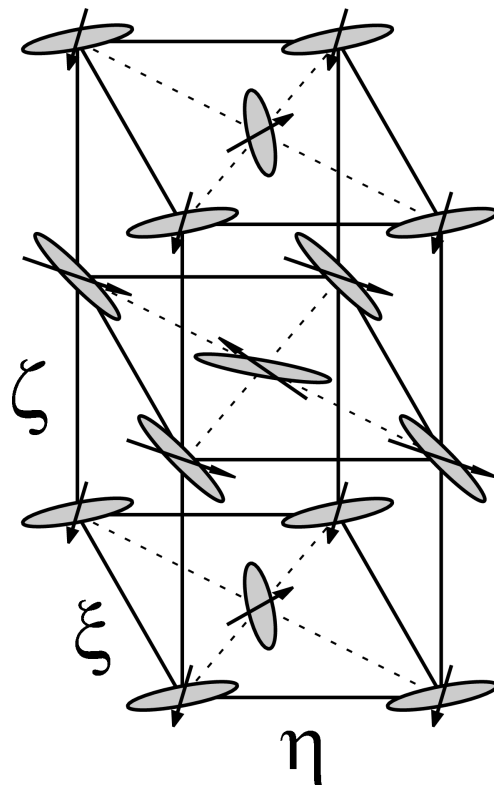


Figure 3

The magnetic structure of DyB₂C₂, showing only Dy atoms and highlighting possible differences in the magnetic and quadrupole canting angles.

The corresponding linear dichroic signal is obtained from (69). For a saturated ion the atomic quantities in (69) are zero apart from $\langle A_{zz} \rangle$ and using in (54) the values $\langle Q_0 \rangle = -15/2$, $\langle P_0 \rangle = 5/2$ and $\langle R_0 \rangle = 0$ we find

$$(3/2)^{1/2} \langle A_{zz} \rangle = -(3/140) \{ -(2\bar{J} + 1) \pm (8/3) \}.$$

Experiments of the type proposed here are very much complementary to studies of forbidden resonant diffraction (e.g. Tanaka *et al.*, 1999; Hirota *et al.*, 2000), which can yield quite direct evidence for quadrupole orbital ordering. The linear dichroism signal in (69) provides, instead, information about the average quadrupole moments: of special interest here might be, for example, any changes observed at the phase transitions. The circular dichroism signal at the $M_{4,5}$ edges depends on the magnetic canting angle. Since the intensity of the forbidden diffraction depends on the orientation of the quadrupole principal axes, a combination of diffraction and circular dichroism data could highlight any differences between the quadrupole and magnetic moment directions. In summary, the experiments described could not only provide strong supporting evidence for the configuration of Dy moments and quadrupole ordering, but would also shed new light on the relationship between quadrupolar and magnetic moment canting angles.

7. Conclusions

Classical optical techniques, including Jones and Mueller calculi, are equally applicable to X-rays and visible light. One can employ such well established techniques to provide a complete description of the passage of X-rays through a material which is anisotropic and magnetic, including all polarization-dependent effects. The scattering amplitude matrix, from which Jones and Mueller matrices can be derived, is related to components of the dipole-dipole tensor. We describe a range of atomic models for these same tensor components, thus providing a complete link between atomic variables and observable quantities in X-ray attenuation and retardation. The chosen example of ferrous niobate illustrates how, armed with the appropriate electronic wavefunction, one can model X-ray attenuation, including linear and circular dichroism. A second example, dysprosium borocarbide, permits us to illustrate the potential value of dichroic signals as a means of unravelling magnetic and orbital ordering.

Because the present treatment is restricted to rank-two tensors, appropriate for pure dipolar events, effects such as natural circular dichroism (Natoli *et al.*, 1998) are not accessible.

APPENDIX A

Some properties of 2×2 square matrices

Let us consider a square matrix of order two,

$$G = \begin{pmatrix} b + a_3 & a_1 - ia_2 \\ a_1 + ia_2 & b - a_3 \end{pmatrix}, \quad (70)$$

where, for the moment, a_1, a_2, a_3 and b are purely real. We note that G is Hermitian and

$$G \equiv bI + \mathbf{a} \cdot \boldsymbol{\sigma}, \quad (71)$$

where I is the unit matrix, and σ_1, σ_2 and σ_3 are standard Pauli matrices defined in (7). In (71) we employ the shorthand notation $\mathbf{a} \cdot \boldsymbol{\sigma} = \sum_j a_j \sigma_j$, $j = 1, 2$ and 3 . The determinant of G is

$$\det G = b^2 - \zeta^2, \quad (72)$$

with $\zeta^2 = \mathbf{a} \cdot \mathbf{a}$, and the trace is

$$\text{tr } G = 2b. \quad (73)$$

Equations (72) and (73) are invariants of G and they are unchanged when G is the subject of a unitary transformation, like a rotation of the axes that span its two-dimensional space.

The two eigenvalues of G are denoted by λ_+ and λ_- and have the values

$$\lambda_{\pm} = b \pm \zeta, \quad (74)$$

which satisfy

$$\det G = \lambda_+ \lambda_-, \quad (75)$$

and

$$\text{tr } G = \lambda_+ + \lambda_-. \quad (76)$$

Using the fact that G satisfies the eigenvalue equation one finds

$$G^2 = 2bG - (b^2 - \zeta^2)I. \quad (77)$$

The corresponding eigenvectors of G are

$$\begin{pmatrix} n_1(\pm) \\ n_2(\pm) \end{pmatrix} \quad (78)$$

with

$$\begin{aligned} n_1(+) &= (a_1 - ia_2)C, & n_2(+) &= (\zeta - a_3)C, \\ n_1(-) &= -(a_3 - \zeta)C, & n_2(-) &= (a_1 + ia_2)C, \end{aligned} \quad (79)$$

in which

$$C = [2\zeta(\zeta - a_3)]^{-1/2}. \quad (80)$$

The two eigenvectors are orthogonal, and each one is normalized to the value 1.

The matrix

$$U = \begin{pmatrix} n_1(+) & n_1(-) \\ n_2(+) & n_2(-) \end{pmatrix} \quad (81)$$

is unitary, $U^+ = U^{-1}$, and satisfies, $U^+ U = I$ and $\det U = 1$. Of course,

$$U^+ G U = \begin{pmatrix} \lambda_+ & 0 \\ 0 & \lambda_- \end{pmatrix} \quad (82)$$

and

$$\begin{aligned} G^{-1} &= U \begin{pmatrix} 1/\lambda_+ & 0 \\ 0 & 1/\lambda_- \end{pmatrix} U^{-1} \\ &= \begin{pmatrix} b - a_3 & -a_1 + ia_2 \\ -a_1 - ia_2 & b + a_3 \end{pmatrix} (b^2 - \zeta^2)^{-1}. \end{aligned} \quad (83)$$

It is interesting to note that the eigenvectors, and hence U , do not depend on b , the coefficient of the unit matrix in (71).

The matrix formed with the symmetrical elements $(1/2)(G_{\alpha\beta} + G_{\beta\alpha})$ is purely real, namely

$$G_s = \begin{pmatrix} b + a_3 & a_1 \\ a_1 & b - a_3 \end{pmatrix}. \quad (84)$$

Let

$$\begin{aligned} \zeta' &= (a_1^2 + a_3^2)^{1/2}, & C'_{\pm} &= [2\zeta'(\zeta' \mp a_3)]^{-1/2}, \\ \cos \varphi &= a_1 C'_+ = (\zeta' + a_3) C'_-, \end{aligned} \quad (85)$$

and

$$\sin \varphi = a_1 C'_- = (\zeta' - a_3) C'_+.$$

Taking $a_2 = 0$ in foregoing results one finds

$$G_s = \begin{pmatrix} \lambda'_+ \cos^2 \varphi + \lambda'_- \sin^2 \varphi & (1/2) \sin(2\varphi)(\lambda'_+ - \lambda'_-) \\ (1/2) \sin(2\varphi)(\lambda'_+ - \lambda'_-) & \lambda'_+ \sin^2 \varphi + \lambda'_- \cos^2 \varphi \end{pmatrix}, \quad (86)$$

with $\lambda'_\pm = b \pm \zeta'$, and

$$\begin{pmatrix} \lambda'_+ & 0 \\ 0 & \lambda'_- \end{pmatrix} = \begin{pmatrix} \cos \varphi & \sin \varphi \\ -\sin \varphi & \cos \varphi \end{pmatrix} G_s \begin{pmatrix} \cos \varphi & -\sin \varphi \\ \sin \varphi & \cos \varphi \end{pmatrix}. \quad (87)$$

The vectors $(\cos \varphi, \sin \varphi)$ and $(-\sin \varphi, \cos \varphi)$ define a set of principal axes in which G_s is diagonal.

The matrix formed with the antisymmetrical elements, $(1/2)(G_{\alpha\beta} - G_{\beta\alpha})$, has two elements and it is purely imaginary. If the elements $\varepsilon_{12} = -\varepsilon_{21} = 1$ define the unit antisymmetrical tensor,

$$(1/2)(G_{\alpha\beta} - G_{\beta\alpha}) = -ia_2 \varepsilon_{\alpha\beta}. \quad (88)$$

For the case in hand, the quantity a_2 is a pseudo-scalar because the rank of the antisymmetrical tensor on the left-hand side of (88) is equal to the dimension of the space in which it is defined. Specifically, the electric field that accompanies a photon is described with two basis vectors (usually called the polarization vectors) and the scattering length, and the density matrix for the states of polarization, are tensors of rank two.

By definition,

$$G = G_s + G_a, \quad (89)$$

and

$$G_a = -ia_2 \begin{pmatrix} 0 & 1 \\ -1 & 0 \end{pmatrix} = a_2 \Sigma. \quad (90)$$

The second equality in (90) defines Σ which is found to be the operator for the helicity of a photon. Note that the matrix representation of Σ is identical to the Pauli matrix σ_2 .

Define angles ψ and η such that

$$\begin{aligned} n_1(+) &= \exp(i\eta) \cos \psi, & n_2(+) &= \sin \psi, \\ n_1(+)/n_2(-) &= -n_1(-)/n_2(+) = \frac{(a_1 - ia_2)}{(a_1^2 + a_2^2)^{1/2}} = \exp(i\eta). \end{aligned} \quad (91)$$

Observe that $\exp(i\eta)$ is the value of the determinant of U defined by (81). One finds,

$$G = \begin{pmatrix} \lambda_+ \cos^2 \psi + \lambda_- \sin^2 \psi & (1/2)e^{i\eta} \sin(2\psi)(\lambda_+ - \lambda_-) \\ (1/2)e^{-i\eta} \sin(2\psi)(\lambda_+ - \lambda_-) & \lambda_+ \sin^2 \psi + \lambda_- \cos^2 \psi \end{pmatrix}, \quad (92)$$

where, as before, $\lambda_\pm = b \pm \zeta$, and now the orthogonality condition is

$$\mathbf{n}(+) \cdot \mathbf{n}^*(-) = 0.$$

In the main text we are led to consider the matrix,

$$\Omega = \exp(G) = \exp(bI) \exp(\mathbf{a} \cdot \boldsymbol{\sigma}). \quad (93)$$

Using $\sigma_j^2 = I$ and $(\mathbf{a} \cdot \boldsymbol{\sigma})^2 = \zeta^2 I$, or (77), one finds for Ω ,

$$\Omega = \exp(b)[I \cosh(\zeta) + \mathbf{a} \cdot \boldsymbol{\sigma} (1/\zeta) \sinh(\zeta)]. \quad (94)$$

This important result is valid for complex \mathbf{a} and b . Note that Ω has exactly the same mathematical structure as G , cf. (71). So, all previous results in Appendix A apply to Ω on making the replacements

$$b \rightarrow \exp(b) \cosh(\zeta) \quad \text{and} \quad \mathbf{a} \rightarrow \mathbf{a} \exp(b) (1/\zeta) \sinh(\zeta). \quad (95)$$

In particular,

$$\text{tr } \Omega = 2 \exp(b) \cosh(\zeta) \quad (96)$$

and

$$\det \Omega = \exp(2b), \quad (97)$$

and if b is purely real it follows from (97) that Ω is a non-singular matrix.

The density matrix for states of polarization in a beam of photons, μ , has the structure of the matrix G , defined in (70) and (71), and \mathbf{a} and b purely real. In this instance,

$$\mu = (1/2)(I + \mathbf{P} \cdot \boldsymbol{\sigma}), \quad (98)$$

where $\mathbf{P} = (P_1, P_2, P_3)$ is the so-called Stokes vector. One sees that $\text{tr } \mu = 1$, and $\det \mu = (1 - P^2)/4 \geq 0$ where $P = (\mathbf{P} \cdot \mathbf{P})^{1/2}$. For a completely polarized beam $P = 1$ and for an unpolarized beam $P = 0$.

Let \mathbf{u} be a unit vector with purely real components $u_j = P_j/P$. Then,

$$\mu = (1/2)(1 - P)I + (1/2)P(I + \mathbf{u} \cdot \boldsymbol{\sigma}), \quad (99)$$

in which the matrix $(I + \mathbf{u} \cdot \boldsymbol{\sigma})/2$ is idempotent, a useful property in manipulations involving μ . A physical interpretation of (99) is that μ is an incoherent mixture of a completely polarized state (often called a pure state, and achieved when a photon is described by a wave function), and a completely unpolarized state.

The average of a quantity Y , say, with respect to the polarization described by \mathbf{P} is

$$\bar{Y} = \text{tr } \mu Y = \text{tr } Y \mu. \quad (100)$$

Taking Y to be a Pauli matrix,

$$\bar{\sigma}_j = P_j. \quad (101)$$

The combination of the three Stokes parameters P_1, P_2 and P_3 into a 'vector' \mathbf{P} is, of course, purely formal and is performed only for convenience of notation. As we have seen, P_2 is a pseudo-scalar, and P_1 and P_3 are true scalars. A second property of the Stokes parameters which demonstrates that \mathbf{P} is not a true vector stems from crossing symmetry. From the latter symmetry one finds the *modulus* of the scattering length is invariant under the transformation expressed by

$$\begin{aligned} E &\leftrightarrow -E', & \mathbf{q} &\leftrightarrow -\mathbf{q}', & P_1 &\leftrightarrow P_1', \\ P_2 &\leftrightarrow -P_2', & P_3 &\leftrightarrow P_3'. \end{aligned} \quad (102)$$

Here, the energy of a photon with wavevector \mathbf{q} is $E = \hbar c|\mathbf{q}|$, and primed quantities relate to the condition of the secondary beam. It is readily shown that, under the reversal of the direction of time, all three Stokes parameters are even.

It is interesting to note that for neutrons and photons the formal mathematical structures of the density matrices are the same. However, the physical significance of \mathbf{P} differs for the two types of particle. In the case of a beam of neutrons \mathbf{P} is twice the mean value of the spin variable for neutrons in the beam. \mathbf{P} , therefore, is odd with respect to the reversal of the direction of time, and a pseudo-vector (also called an axial vector). Thus, under the parity transformation, which inverts spatial coordinates and so changes a right-handed system of coordinates to a left-handed system of coordinates and *vice versa*, the polarization of neutrons is unchanged. Under the parity transformation, the Stokes parameters P_1 and P_3 are unchanged, whereas P_2 , the mean helicity, changes its sign, *i.e.* P_1 and P_3 are true scalars and P_2 is a pseudo-scalar. The change in sign of P_2 is evident from its relation to helicity, the operator for which is the scalar product of a polar vector (the photon wavevector) and an axial vector (the photon spin). With regard to spatial symmetries for the two types of particles it is relevant that the symmetry group for the density matrix of photons is $\text{SO}(2)$, while for neutrons the symmetry group is $\text{SU}(2)$, of course. For one thing, the dimension of $\text{SO}(2)$ equals the

rank of the density matrix and, from this alone, we have noted that the Stokes parameter P_2 is a pseudo-scalar.

We have benefited from discussions with Dr S. Langridge, Dr U. Staub and Dr Y. Tanaka. Dr K. S. Knight collaborated on the calculations for dysprosium borocarbide reported in §6.

References

- Begum, R., Hart, M., Lea, K. R. & Siddons, D. P. (1986). *Acta Cryst.* **A42**, 456–464.
- Berestetskii, V. B., Lifshitz, E. M. & Pitaevskii, L. P. (1982). *Quantum Electrodynamics*. Oxford: Pergamon Press.
- Birss, R. R., (1964). *Symmetry and Magnetism*. Amsterdam: North-Holland.
- Brosseau, C. (1998). *Polarized Light*. New York: John Wiley.
- Carra, P. & Thole, B. T. (1994). *Rev. Mod. Phys.* **66**, 1509–1515.
- Collins, S. P. (1999). *J. Phys. Condens. Matter*, **11**, 1159–1175.
- Crocombette, J. P., Thole, B. T. & Jollet, F. (1996). *J. Phys. Condens. Matter*, **8**, 4095–4105.
- Gel'mukhanov, F. & Ågren, H. (1999). *Phys. Rep.* **312**, 87–330.
- Heid, C., Weitzel, H., Bourdarot, F., Calemczuk, R., Vogt, T. & Fuess, H. (1996). *J. Phys. Condens. Matter*, **8**, 10609–10625.
- Hirota, K., Oumi, N., Matsumura, T., Nakao, N., Wakabayashi, Y., Murakami, Y. & Endoh, Y. (2000). *Phys. Rev. Lett.* **12**, 2706–2709.
- Jones, R. C. (1948). *J. Opt. Soc. Am.* **38**, 671–685.
- Judd, B. R. (1962). *Phys. Rev.* **127**, 750–761.
- Laan, G. van der (1994). *J. Phys. Soc. Jpn*, **63**, 2393–2400.
- Landau, L. D. & Lifshitz, E. M. (1977). *Quantum Mechanics*. Oxford: Pergamon.
- Landau, L. D., Lifshitz, E. M. & Pitaevskii, L. P. (1984). *Electrodynamics of Continuous Media*. Oxford: Pergamon.
- Loudon, R. (1983). *The Quantum theory of Light*. Oxford: Clarendon.
- Lovesey, S. W. & Balcar, E. (1997). *J. Phys. Condens. Matter*, **9**, 4237–4260; 8679–8692.
- Lovesey, S. W., Fritz, O. & Balcar, E. (1998). *J. Phys. Condens. Matter*, **10**, 501–524.
- Lovesey, S. W. & Grimmer, H. (1997). *J. Phys. Condens. Matter*, **9**, 4261–4269.
- Mandel, L. & Wolf, E. (1995). *Optical Coherence and Quantum Optics*. Cambridge University Press.
- Natoli, C. R., Brouder, C. H., Saintavit, P., Goulon, J., Goulon-Ginet, Ch. & Rogalev, A. (1998). *Eur. Phys. J.* **B4**, 1–11.
- Nye, J. F. (1960). *Physical Properties of Crystals*. Oxford: Clarendon.
- Ofelt, G. S. (1962). *J. Chem. Phys.* **37**, 511–520.
- O'Handley, R. C. (2000). *Modern Magnetic Materials*. New York: John Wiley.
- Saintavit, P., Arrio, M.-A. & Brouder, C. (1995). *Phys. Rev. B*, **52**, 12766–12769.
- Schwarzenbach, D. (1996). *Crystallography*. Chichester: John Wiley.
- Swindell, W. (1975). *Benchmark Papers in Optics/1*. Stroudsburg, PA: Dowden, Hutchinson and Ross.
- Tanaka, Y., Inami, T., Nakamura, T., Yamauchi, H., Onodera, H., Ohoyama, K. & Yamaguchi, Y. (1999). *J. Phys. Condens. Matter*, **11**, L505–511.
- Thole, B. T., Carra, P., Sette, F. & van der Laan, G. (1992). *Phys. Rev. Lett.* **68**, 1943–1946.
- Varshalovich, D. A., Moskalev, A. N. & Khersonakii, V. K. (1988). *Quantum Theory of Angular Momentum*. Singapore: World Scientific.
- Yamauchi, H., Onodera, H., Ohoyama, K., Onimaru, T., Kosaka, M., Ohashi, M. & Yamaguchi, Y. (1999). *J. Phys. Soc. Jpn*, **68**, 2057–2066.